Peer-reviewed version available at *Materials* **2020**, *13*, 1636; doi:10.3390/ma13071636

*Article*

# Direct ink writing glass: a preliminary step for optical application

**Bo Nan [1,2,§], Przemysław Gołębiewski [3,4,§], Ryszard Buczyński [3,4], Francisco J. Galindo-Rosales [5] and José M. F. Ferreira [1,*]**

[1] Department of Materials and Ceramic Engineering, University of Aveiro, CICECO – Aveiro Materials Institute, 3810-193 Aveiro, Portugal; jmf@ua.pt
[2] CEITEC - Central European Institute of Technology, Brno University of Technology, Purkynova 656/123, 612 00 Brno, Czech Republic; Bo.Nan@ceitec.vutbr.cz
[3] Institute of Electronic Materials Technology, Wólczyńska 133, 01-919 Warsaw, Poland; przemyslaw.golebiewski@itme.edu.pl
[4] Faculty of Physics, University of Warsaw, Pasteura 5, 02-093 Warsaw, Poland, ryszard.buczynski@fuw.edu.pl
[5] CEFT, Department of Chemical Engineering, Faculty of Engineering of the University of Porto, 4200-465 Porto, Portugal; galindo@fe.up.pt

§ These two authors contribute equally.
* Correspondence: jmf@ua.pt; Tel.: + 351 234 370 354

**Abstract:** In this paper, we present a preliminary study and conceptual idea concerning 3D printing water-sensitive glass by exemplifying with a borosilicate glass with high alkali and alkaline oxide contents using direct ink writing. The investigated material was prepared in the form of a glass frit, which was further ground in order to obtain a fine powder of desired particle size distribution. In a following step, inks were prepared by mixing the fine glass powder with Pluoronic F-127 hydrogel. The acquired pastes were rheologically characterized and printed using a Robocasting device. DSC experiments were performed for base materials and the obtained green bodies. After sintering, SEM and XRD analyses were carried out in order to examine microstructure and the eventual presence of crystalline phase inclusions. Results confirmed that obtained inks exhibit stable rheological properties despite the propensity of glass to undergo hydrolysis and could be adjusted to desirable values for 3D printing. No additional phase was observed, supporting the suitability of the designed technology for the production of water sensitive glass inks. SEM micrographs of the sintered samples revealed the presence of closed porosity, which may be the main reason of light scattering.

**Keywords:** direct ink writing, glass, rheology

## 1. Introduction

After almost thirty years of development, additive manufacturing, or commonly named 3D printing, has started to play an important role in the modern industry such as automobile, aerospace, bioengineering, etc., and the interest of research still maintains enthusiasm [1-5]. It is not only a near-net shaping but also a moldless shaping method, which can be readily categorized into two different types, namely light-based and ink-based 3D printing [6], or into seven different types, according to the classification of American Society for Testing and Materials (ASTM) 52900:2015 standard [1]. Among those advanced techniques, most of the researches have been focused on metals, ceramics or polymers [7-11], while only a few attempts are applied in shaping glass.

Similar to many materials that are hard to machine, the difficulty of shaping glass lies in the material itself, as it is brittle and usually sensitive to thermal shock. Many types of glasses are also prone to crystallization upon reheating which makes processing temperature range limited. Moreover, it can be difficult to apply shaping techniques for glasses that are based on powder densification, as the main issue is its behavior in elevated temperatures. Unlike sintering ceramics or

metals, a glass starts to flow as a viscous material after reaching the transition temperature. As a result, it is challenging to retain shape of already formed object while sintering process is applied, otherwise a very precise control of temperature and dwelling time is needed. Apart from the solid-state processing, colloidal shaping processes require well-dispersed suspensions. However, the complex compositions of various types of glasses may undergo preferential ionic leaching of certain components in the dispersing liquid that affect the homogenization of the dispersed system. Such compositions commonly consist of not only glass-forming compounds but also additives to either modify final parameters of glass or to reduce manufacturing cost. Taking the water-based system as an example, alkaline earth and alkali oxides such as $Na_2O$, which is aimed to lower the operating temperature range for silica-based glasses, may be hydrolyzed, leading to the alteration of rheological properties of the suspension and further inhibiting the liquid processing, as a result of pH change in the glass suspensions with time. Although using non-aqueous suspension can eliminate the dissolving or hydrolyzing problems, the organic liquids are usually toxic and more expensive. Therefore, research on liquid processing glass, especially connected with additive manufacturing, focuses mainly on silica-rich [12-13] and bioactive glasses [14-15], as the first type is more resistant to thermal shock and allows the production of dense and transparent samples, and the latter type is preferred in porous scaffold formed to enhance its bioactivity and osteointegration potential.

Since 3D printing is a readily accessible shaping method and has been utilized in many kinds of materials, it may be still a good candidate for shaping glass as well. Recent reports have brought excellent examples and gained confidence in both glass and 3D printing community by various methods such as depositing and annealing the molten filaments, laser aided filament-fed process, direct ink writing, stereolithography and digital light processing [12-13, 16-19]. Among them, the first two require high energy source such as heating or laser assisted printing, with the glass being prepared in one step, while at least two steps were required for the other methods, i.e. green glass samples were printed with an extra follow-up sintering process. Although it seems that one-step procedure is an easy option, it involves very precise control of temperature and expensive assisting parts to guarantee the stability of the printing process. For printing in more steps, it is easy to obtain more broad compositions and increase the resolution of the as-designed geometry by utilizing and changing the formulation of the liquid molecular precursor, being economically applicable for a small batch of samples at a laboratory level. The comparison of these reported methods can be found in Table 1.

**Table 1.** Comparison of reported printing methods.

| Method | Procedure | Printing precursor(s) | Light/Ink based | Nozzle | References |
|---|---|---|---|---|---|
| Molten filament deposition | One step | Molten glass | Ink based | Yes | [18] |
| Laser aided filament deposition | One step | Glass filament | Both | Yes | [19] |
| Direct ink writing | More steps | Suspension of nanoparticles /Sol–gel derived feedstock | Ink based | Yes | [12, 14-16] |
| Stereolithography | More steps | Curable monomer with nanopowder | Light based | No | [13] |
| Digital light processing | More steps | Alkoxide precursors, photoactive monomer and light-absorbing dye | Light based | No | [9, 17] |

Here, we report a preliminary experiment on printing borosilicate glass by direct ink writing. Unlike the previous reports in [12,16], the micron-sized borosilicate glass particles are utilized instead of the nanoparticles or liquid molecular precursors (sol-gel) of silica or silica-based compositions. The first challenge is to form colloidal stable inks as the borosilicate glass used in this study undergoes hydrolysis which, as it was mentioned before, makes suspension rheologically unpredictable. In this study, we proposed an ink prepared by dispersing glass powder in the Pluronic F-127 hydrogel.

Peer-reviewed version available at Materials 2020, 13, 1636; doi:10.3390/ma13071636

Pluronic F-127 is a triblock copolymer of polyethylene oxide-polypropylene oxide-polyethylene oxide (PEO-PPO-PEO). Because of the hydrophilic nature of PEO and hydrophobic nature of PPO, Pluronic exhibits amphiphilic behavior. As a result of hydrophobic effect described in [20], after reaching a certain concentration named critical micelle concentration (CMC), it starts to form micelles, typically in a spherical shape. In addition, this hydrophobic effect corresponds to an increase of entropy. It implies that an increase in temperature will result in a higher degree of micellization. The gel is formed because of the increasing volume of the micelles and repulsive forces between them [21]. In previous studies, Bromberg et al. [22] and Park et al. [23] reported that Pluronic hydrogels are stable, while the pH of solution is changed. Based on this data, it is assumed that the stability of hydrogel-based suspensions should increase significantly in comparison to other ionic strength sensitive dispersing liquids, thus facilitating the printing of water-sensitive glass materials. The second challenge is related to the thermal treatment processes: debinding (burnout of organic substances present in the printed sample) and sintering, which should result in obtaining denser and more transparent printed samples. If both challenges are overcome, then it will be possible to print more complex shapes, e.g. preforms for optical fiber production.

## 2. Materials and Methods

### Preparation of glass powder

The borosilicate glass considered in this study was prepared in the form of frit. Fine powders: $SiO_2$ (milled fused silica, Lianyungang DIGHEN Composite Material Technology Co.,Ltd, China), $H_3BO_3$ (Chempur, Poland, ≥99,5%), MgO (Chempur, Poland, ≥98%), $CaCO_3$ (Chempur, Poland, ≥ 99%), $Na_2CO_3$ (Chempur, Poland, ≥ 98,8%), $KNO_3$ (Chempur, Poland, ≥ 99%), $K_2CO_3$ (Chempur, Poland, ≥ 99%) were used as raw materials. The composition of fabricated glass is presented in Table 2.

**Table 2.** Chemical compositions of glass powder.

| Compound | $SiO_2$ | $Al_2O_3$ | $B_2O_3$ | MgO | CaO | $Na_2O$ | $K_2O$ |
|---|---|---|---|---|---|---|---|
| **mole %** | 62.5 | 2.0 | 11.5 | 7.0 | 4.0 | 3.5 | 9.5 |

Calculations were made in order to obtain 750 g of glass frit. In the first step, proper amounts of raw materials were mixed using alumina mortar. Obtained mixture was transferred to platinum crucible which was preheated to 1250°C in the furnace. Afterwards the batch was melted at 1370°C for 3 h. During melting process, the batch was mixed 3 times using silica rod. In the next step, melt was cast into cold water. As-cast frit was separated from water and dried in the oven at 60°C for 24 h. Subsequently, received material was mechanically crushed into smaller pieces using alumina mortar as well as it was milled in a planetary mill (PM) using agate container and balls (mixture of different sizes, ball-to-powder ratio of 2:1). Small portions of powder after 2, 4 and 6 h of planetary milling were collected. Finally, glass was attrition milled (AM) in ethanol (zirconia balls with 3 mm diameter and the ball-to-powder ratio of 3:1) at the rate of 500 rpm for 3 h, to further break the large particles into smaller ones. After three hours, small portion of suspension was collected and dried at 80°C overnight. Particle size and particle size distributions of gathered borosilicate glass powders were determined using a laser diffraction analysis (Coulter LS 230, UK). A given amount of powder (~0.3 g) was dispersed in 50 mL of deionized water with the aid of a drop of Dolapix CE64 (ZSCHIMMER & SCHWARZ, Germany). The dilute suspension was sonicated for 5 mins to destroy the agglomerates before performing the particle size and particle distribution measurements. Finally, suspension after attrition milling was dried at 80°C overnight and passed through a 40 μm polymer sieve.

### Ink preparation

The glass inks for direct ink writing were prepared by following several successive steps as depicted in Fig. 1. Before preparing glass inks, Pluronic F-127 (Sigma-Aldrich, Darmstadt, Germany) was dissolved into deionized water with concentrations of 10, 20, 30, 40 and 50 wt.%, respectively. The mass of the chemicals was weighed in a high-accuracy (0.0001 g) weighing scale. All the polymer solutions were

Preprints (www.preprints.org) | NOT PEER-REVIEWED | Posted: 10 March 2020 doi:10.20944/preprints202003.0169.v1

Peer-reviewed version available at Materials 2020, 13, 1636; doi:10.3390/ma13071636

kept in hermetic containers to prevent water evaporation, and stored in fridge (~4 °C) overnight, to further homogenize the composition.

Glass inks with a series of solids loading of 15.0, 25.0 and 35.0 wt.% were prepared by mixing the as-milled glass powder with the Pluronic stock solution (30 wt.%) in a planetary mixer (THINKY ARE-250, Japan). The powder was gradually added into the polymer solution, followed by stirring at the rate of 1500 rpm till all the objective amount of the powder has been incorporated. During each mixing interval, the as-mixed suspension was immediately taken out from the mixer and kept into an iced water tank to get it cooled down for 3 minutes. Contrasting to the preparation procedures previously reported, involving the successive mixing steps after adding each kind of processing additive (dispersant-binder-coagulant) [24-26], the one-step mixing utilized in this study simplifies and facilitates the preparation of the inks. The final as-mixed suspension was sonicated for 5 minutes to destroy the possible agglomerates prior to any further use.

**Rheological tests**

The viscoelastic properties of the Pluronic F-127 solutions and glass inks were characterized by a stress-controlled rotational rheometer (Anton Paar MCR301, Austria) equipped with a Dynamic Shear Stress CSS rotational module and a direct strain oscillatory module (DSO). Steady state flow curves were obtained by imposing a logarithmic ramp in shear stress. The limits of the linear viscoelastic region (LVE region) were determined by means of amplitude strain sweep experiments at the constant frequency of 1.0 Hz. Additionally, three interval thixotropy tests (3ITT) were developed in order to determine if the samples are prone to recovery quickly the gel state after being sheared at large deformations, which is paramount for ensuring the shape retention of the extruded filaments [27]. The 3ITT experiments consisted of three concatenated oscillatory shear deformation steps at a constant frequency of 1.0 Hz: The first interval consisted of an of 0.005% during 120 seconds; the second step at 500% for 120 seconds; and the third interval at the same deformation of the first one during 600 seconds. Based on the result obtained from amplitude sweep experiments, oscillations with amplitude of deformation of 0.005% were within the LVE region, while a shear strain of 500% was in the non-linear viscoelastic region.

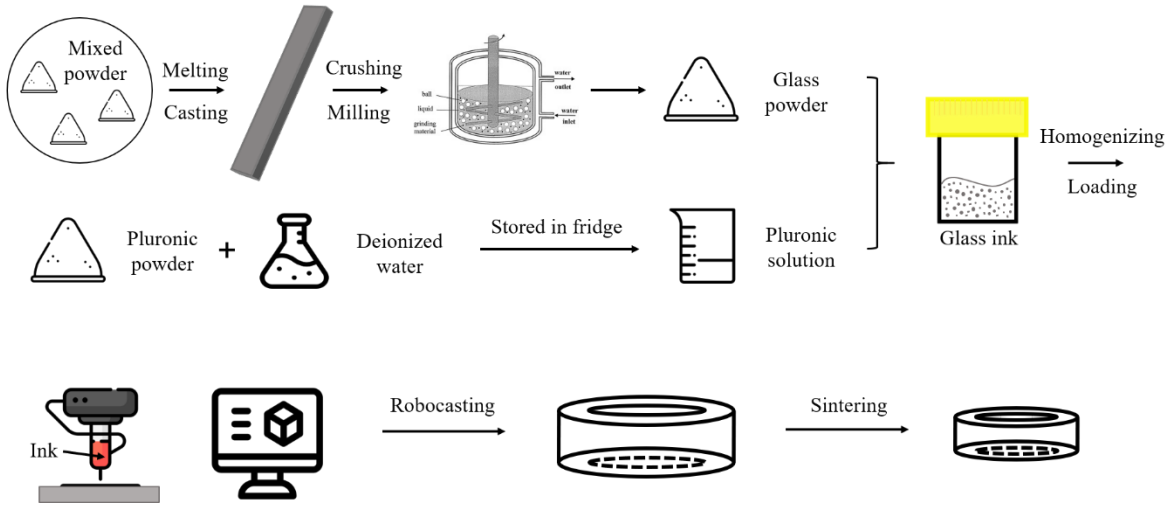


**Figure 1.** Schematics of glass ink preparation.

To minimize the possible slipping effect, measurements were performed with a serrated plate-and-plate (PP10/P2, Anton Paar, Austria) with a gap of 0.4 mm. The temperature was set at 25°C and controlled with a built-in Peltier system, and a solvent trap cover was used to prevent a partial evaporation of the solvent from the samples during the tests.

**Direct ink writing**

Three kinds of as-prepared ink (with solids loading of 15, 25 and 35 wt.%) were loaded into syringes (Luer locker, 3 ml, Nordson, USA) and extruded through the same nozzle (Optimum® general purpose

dispense tips, internal diameter 250 µm, Nordson, USA). The hollow cylinder geometry was designed by a CAD software (FreeCAD, version 0.18) and sliced by Robocad software attached to the Robocasting system (Model EBRD-A32, 3D Inks, LLC, USA). The details of equipment and its related accessories utilized during experiments are shown in Fig. 2. Before printing, the printing atmosphere (temperature ~25°C and relative humidity ~80 %) was adjusted by an air humidifier (SHF 911GR, Sencor, Japan) and monitored by a thermo-hygrometer (NK-TH2, NKTECH, China). The syringe driver dispensed the ink on an aluminum oxide substrate (surface spread with a thin layer of anti-stick agent, 100 × 100 × 1 mm, Zhengzhou Kejia Furnace CO., LTD, China). After printing each sample, the substrate was transferred immediately into a homemade box with wet tissue inside and dried in a preheated oven at 80°C till the samples got dried and hardened. The samples could be easily detached from the substrate after drying, and the greasy anti-stick layer and Pluronic could be removed by further firing process, with the ramp rate 1°C/min up to 500°C holding at this temperature for 2 hours.

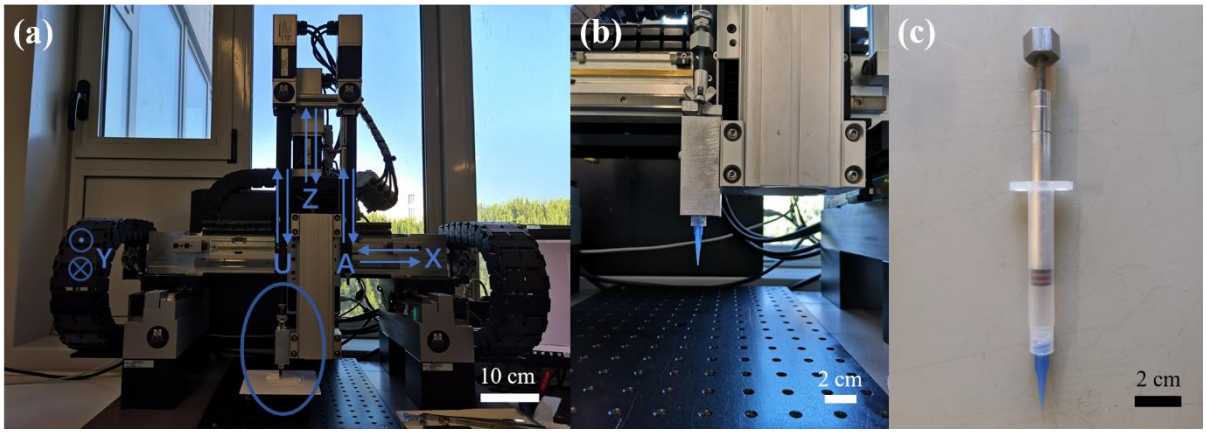


**Figure 2.** Facility of direct ink writing: (a) the Robocasting machine (b) enlarged parts (left syringe chamber) as labelled in (a) and (c) a 3 mL syringe with a 410 µm nozzle.

**Differential scanning calorimetry coupled with thermogravimetry (DSC/DSC-TG)**

To evaluate suitable parameters for debinding and sintering processes of printed glass samples, differential scanning calorimetry coupled with thermogravimetry was performed. Green body received after printing and drying was crushed and ground in agate mortar to obtain a powder. Measurement was carried out in alumina crucible in the temperature range from 25°C to 1100°C at a heating rate of 10°C/min using Netzsch STA 449F1 calorimeter. Second alumina crucible was used as a reference. Measurements of glass frit and pure Pluronic F-127 were also made to distinguish processes corresponding to each material. In case of Pluronic F-127, the measurement was carried out with slower heating rate equal to 2°C/min up to 1000°C. All above measurements were performed in "synthetic air" atmosphere with the composition of 80 vol.% of Ar and 20% of $O_2$.

**Sintering**

After drying, printed samples were fired in a two-step process according to the results obtained from DSC-TG measurement. Firstly, samples were debinded at 500°C for 8 h (heating rate 30°C/h) and afterwards sintered at 720°C (heating rate 150°C/h) for 30 min.

**X-ray powder diffraction (XRD)**

In order to determine the presence of crystalline impurities introduced during samples elaboration, especially during milling process (quartz or/and zirconia), XRD measurement of the sintered glass sample (crushed and ground to obtain fine powder) was performed. In this study, Bruker D8 Advance X-ray diffractometer was used. Measurement was carried out in symmetric geometry, with Cu anode ($\lambda_{CuK\alpha}$=1.5418 Å) using Lynx Eye type high efficiency linear detector. Sample was tested in 2θ~10–100° at a step rate of 0.02° and dwelling time equal to 2 s.

## 3. Results

Fig. 3 and Table 3 present particle size distributions of glass powders obtained after different milling times. Sample collected after 2 hours of planetary milling cannot reach necessary signal threshold, which means that the milling time was insufficient and the size of most particles is still too high. One can observe that increasing the time of milling gradually results in smaller particle sizes with narrower distributions. After 4 h of planetary milling, a broad plateau from 4 to 40 μm can be identified. Subsequent milling for additional 2 hours results in a bimodal particle size distribution with two maxima at around 3 and 20 μm. Finally, after applying attrition milling, the powder starts to show almost unimodal distribution with $d_{50}$ = 4.2 μm. Moreover, $d_{10}$ and $d_{25}$ values remain at a similar level for the whole milling time, while $d_{90}$ values diminish over 3 times. This means that milling process under such a condition does not significantly affect particles with size below 2 μm.

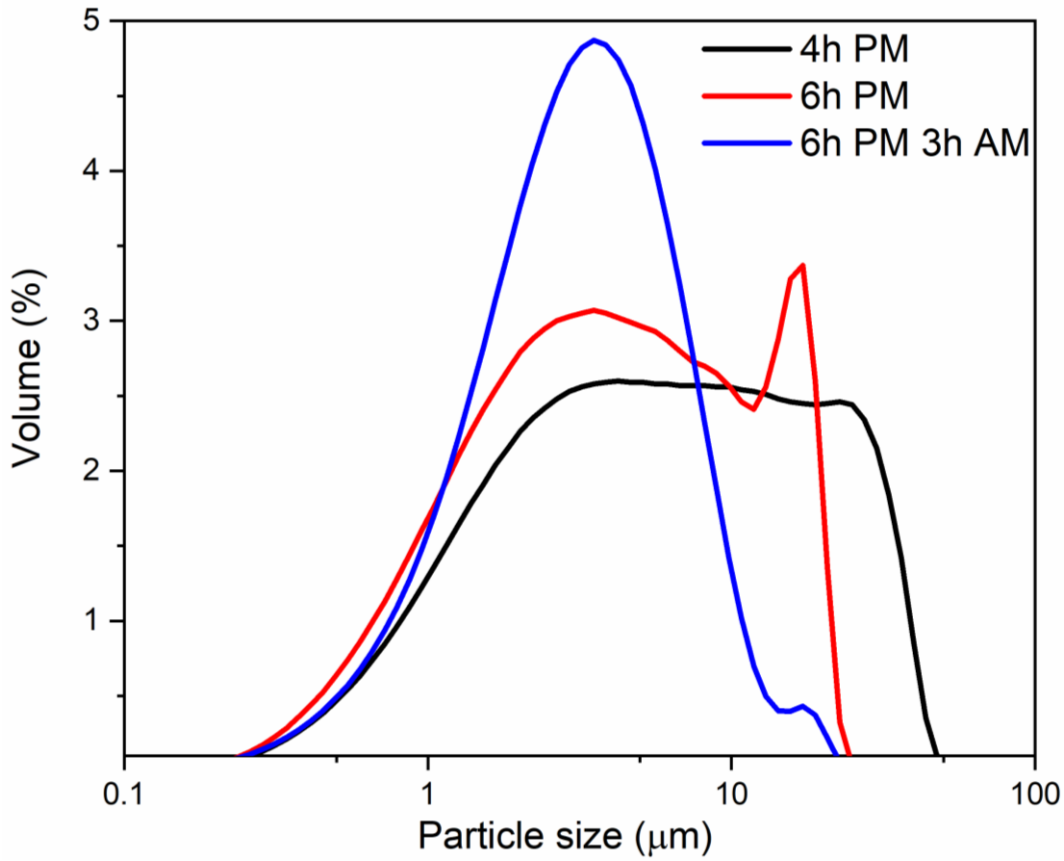


**Figure 3.** Particle size distributions of glass powders after different time of milling. Black line (4h PM) corresponds powder milled in planetary mill for 4 h, green line (6h PM) corresponds to 6 h of planetary milling, blue line (6h PM, 3h AM) corresponds to powder obtained after 6 h of planetary milling followed by 3 h of attrition milling.

Preprints (www.preprints.org) | NOT PEER-REVIEWED | Posted: 10 March 2020 doi:10.20944/preprints202003.0169.v1

Peer-reviewed version available at Materials 2020, 13, 1636; doi:10.3390/ma13071636

**Table 2.** Particle size distribution after different time of milling.

| Sample | Particle size distribution (μm) | | | | |
|---|---|---|---|---|---|
| | $d_{10}$ | $d_{25}$ | $d_{50}$ | $d_{75}$ | $d_{90}$ |
| **4 h PM** | 1.2 | 2.4 | 6.0 | 15.2 | 26.7 |
| **6 h PM** | 1.0 | 1.9 | 4.2 | 9.4 | 16.1 |
| **6 h PM, 3 h AM** | 1.1 | 1.9 | 3.3 | 5.3 | 7.8 |

Preliminary experiments were firstly carried out using the common approach for preparing inks comprising three processing additives, i.e. anionic dispersant, thickener and cationic coagulant. However, soon it became clear that this approach could not be successfully applied to this glass system. The electrostatic interactions between an anionic dispersant and a cationic coagulant, like polyethyleneimine (PEI), are maximum within the neutral pH region. As the tendency of the glass powder to hydrolyze is high, the alkaline earth and alkali ions leached to the dispersing water make the pH of the suspension to increase to high values at which the PEI species exist essentially in the non-dissociated form, thus preventing the coagulation phenomenon to occur [15]. Under such conditions, the stiffness of the ink is insufficient to grant shape retention to the extruded filaments, and the as-printed layers are not mechanically strong to support the consecutively deposited layers while building up the part. Instead, the gelation of Pluronic F-127 is driven by the temperature dependent hydrophilic–hydrophobic interactions [20-21], which are less sensitive to ionic strength of the dispersing liquid. This is to say that the rheological behavior of glass powder inks prepared with Pluronic hydrogel is not much affected by glass hydrolysis. Another advantage of using Pluronic hydrogel, which does not involve the addition of processing additive solutions inevitably causing a diluting effect, is the easiness of how the required solids volume fraction can be accurately adjusted and controlled.

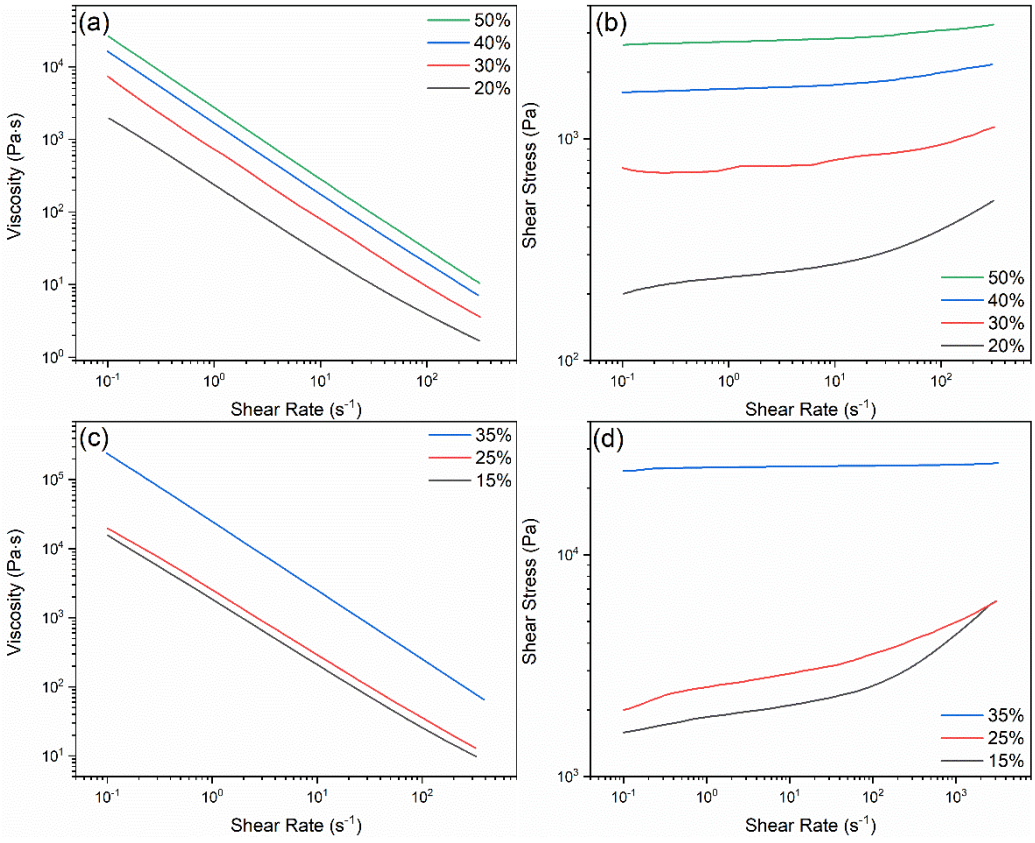


**Figure 4.** Flow curves and shear stress vs. shear rate curves of (a) (b) Pluronic solutions and (c) (d) glass inks of different solids loadings prepared in the 30 wt.% Pluronic stock solution.

Pluronic solutions with five different concentrations were prepared. They can readily liquify at a low temperature and jellify again when placed at room temperature [28]. The solution with 10 wt.% Pluronic is able to flow even at room temperature, being therefore improper for further glass ink gelation and printing, and that is why it was not tested on rheometer. Fig. 4 depicts the results of flow curves measured for both pure Pluronic solutions and glass inks. With an increasing concentration, the viscosity of the Pluronic solutions and of the glass inks increases, respectively, from $2\times10^3$ Pa·s to $3\times10^4$ Pa·s at a low shear rate of $10^{-1}$ $s^{-1}$; and from $2\times10^4$ Pa·s to $3\times10^5$ Pa·s at $10^{-1}$ $s^{-1}$, as shown in Fig. 4(a) and 4(c). The shear rate-shear stress curves (Fig. 4(b) and 4(d)) reveal that the curves become flatter with increasing concentrations of both Pluronic and glass in the inks, as a mechanically percolating and space filling network is developed, which is characteristic of a solid like material. The yield stress can be calculated by extrapolating to zero shear rate the steady-state flow curve [29]. The higher concentration of the solutions/suspensions will increase the yield stress. In the real printing process, it reflects the shear stress/strain applied in the syringe to start the flow of the gelled solutions/suspensions.

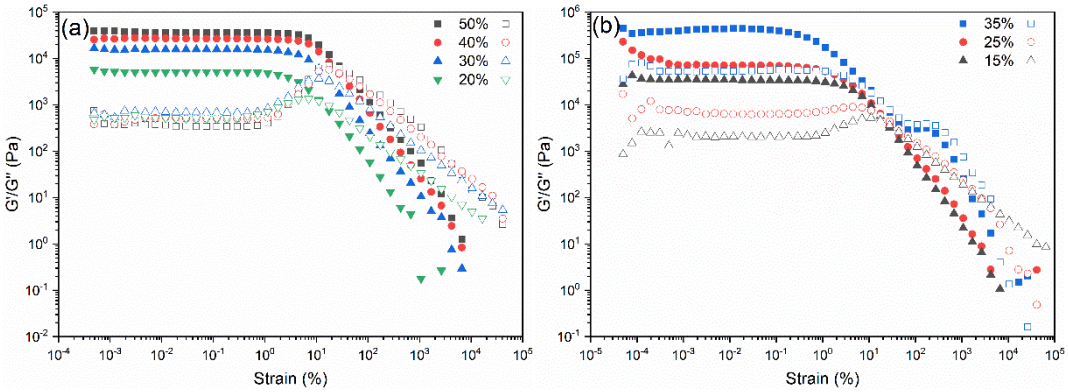


**Figure 5.** Linear viscoelastic region (LVR) of (a) Pluronic solutions and (b) glass inks measured under amplitude sweep mode. The elastic modulus (G') and viscous modulus (G'') are labelled as solid dots and empty symbols, respectively.

Further measuring Pluronic solutions and glass inks in oscillatory mode allows to observe that by increasing the percentage of Pluronic, the network becomes more flexible; however, for a fixed concentration of Pluronic, the larger the concentration of solid loading, the more brittle the network of the glass ink, reflected by lower critical strains. Moreover, the values of elastic modulus (G') grow with the increasing concentrations of both polymer solutions and glass inks, which agrees with the results obtained in the steady shear experiments. It is also worth mentioning that the cross-over points of G' and G'' curves in Pluronic solutions change from 10% to 27%, while for the glass inks, they change from 27% to 17%, which have the converse trends, as shown in Fig. 5. It means that the critical shear strain to break the gelled structure to flow is getting larger with the increasing concentrations of polymer, as more micelles in the system are, the more the network before losing its structure can deform. For the glass inks, the critical shear strain to break the ligation between the polymer and glass particles is decreasing with the increasing concentration of glass, because the glass particles are distributed homogeneously in the polymer solutions and the bonding is weaker between the particles and polymer chains than that among the polymer micelles, with a greater number of particles introduced, causing the critical shear strain decrease. Different from the previous reports of the ink system consisting of dispersant – HPMC – PEI in [30], where a strain thinning behavior (type I) is shown, the ones of Pluronic solutions and glass inks exhibit a weak strain overshoot behavior (type III) [30], and their corresponding chain structures can be found in [31]. The different structures lie in the homogeneity of the as-mixed ink caused by the discrepancy of the particle size, i.e. the glass powder still has larger particles than those in ceramic powder. Therefore, the oscillatory mode can offer more information than the rotational counterpart.

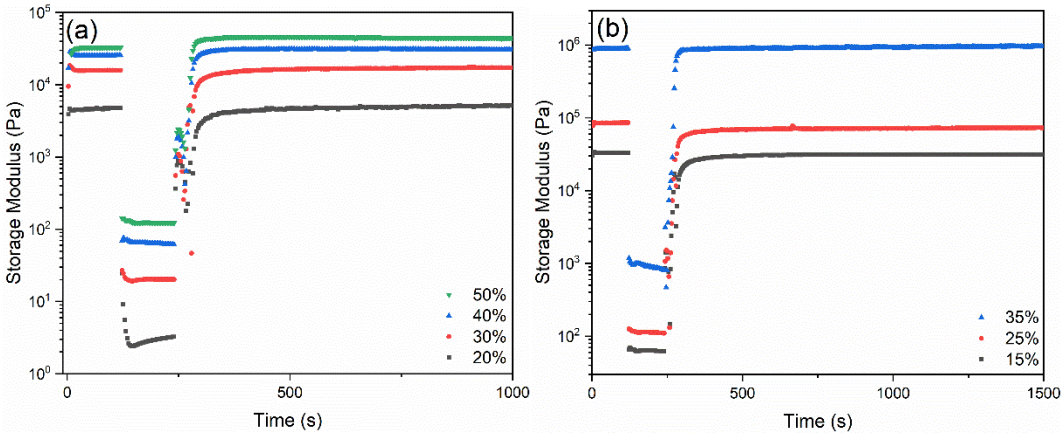


**Figure 6.** Three interval thixotropy test (3ITT) results describing changing structures of (a) Pluronic solutions and (b) glass inks.

As mentioned above, the common dispersant-thickener-coagulant system is not applicable for 3D printing, due to the insufficient stiffness of the as-printed layers for supporting the weight of the consecutive layers. The reason for this phenomenon is account for lacking ability to fast recover the gelled structure from the deformed state observed in the common ink system. In Fig. 6, in order to analyze the change of the internal structure, the thixotropic behavior of both Pluronic solutions and glass inks are characterized in terms of the viscoelastic moduli by means of the three interval thixotropy test (3ITT) [31-34]. According to the results in Fig. 5, where the shear strain spans from linear region to non-linear region, the input shear strain signal was chosen as 0.005% and 500%, respectively. For Pluronic solutions, in the first deformation step within the linear viscoelastic region (LVR), the G′ values are constant, which simulates the structure is stable when the solutions/inks are not compressed. Then, the deformation enters into the non-linear region, as G′ immediately decreases, due to the breakdown of the internal structure of the solutions/inks, simulating the printing process when the solutions/inks are under pressure. Subsequently, when the shear strain decreases back again to 0.005%, G′ gradually increases, as the internal structure recovers to the original gelled one when left standing, depicting the structural change in the as-printed filaments when attached to the substrate. The results from Pluronic solutions show good recovering ability, as G′ can reach 100% after sheared in non-linear region. The glass inks inherit this excellent recovery behaviour from the Pluronic solutions, where G′ can rebuild up to 73.9%, 71.1% and 97.2% after being sheared under 500% and the structure is left undeformed for 81 seconds, in terms of the increasing solids-loadings of the ink. When the solids-loading is 35 wt.% in the glass ink, it can even recover faster than the ones with the common dispersant-thickener-coagulant system reported previously [34].

Fig. 7 presents DSC/TG curves of glass frit (a), printed sample (b) and pure Pluronic F-127 (c). In Fig. 7a and 7b, one can see a drop of a heat flow in the temperature range below 50°C. It is connected to higher inertia of the crucible with sample in comparison with reference. Reasons are ascribed to the high amount of powder specimen (around 50 mg) and high heating rate. DSC curve of pure polymer (Fig. 7c) does not exhibit similar behavior because of slower heating rate. Measurement of pure glass frit revealed 3 inflection points above 500°C. The first one at around 560°C and second one at 690°C may correspond to glass transition temperature ($T_g$) which means that produced material is phase separated. The third inflection point at around 860°C may represent slow reaction occurring between glass sample and crucible material. In case of printed sample, one can observe endothermic peak at around 60°C corresponding to the melting of Pluronic F-127 as it is also evident on DSC curve of pure polymer. Strong exothermic peak at around 200°C visible in both Fig. 7b and 7c is an effect of polymer thermal decomposition. In contrary to Fig. 7a and 7c, the printed sample exhibits additional exothermic peak at around 310°C. The most conceivable explanation is that printed sample contains also residue of polytetrafluoroethylene which is used as construction material of attrition mill container. According to the DSC measurements, debinding temperature was set at 500°C for best possible burnout of organics without allowing glass to flow over its $T_g$.

Preprints (www.preprints.org) | NOT PEER-REVIEWED | Posted: 10 March 2020 doi:10.20944/preprints202003.0169.v1

Peer-reviewed version available at Materials 2020, 13, 1636; doi:10.3390/ma13071636

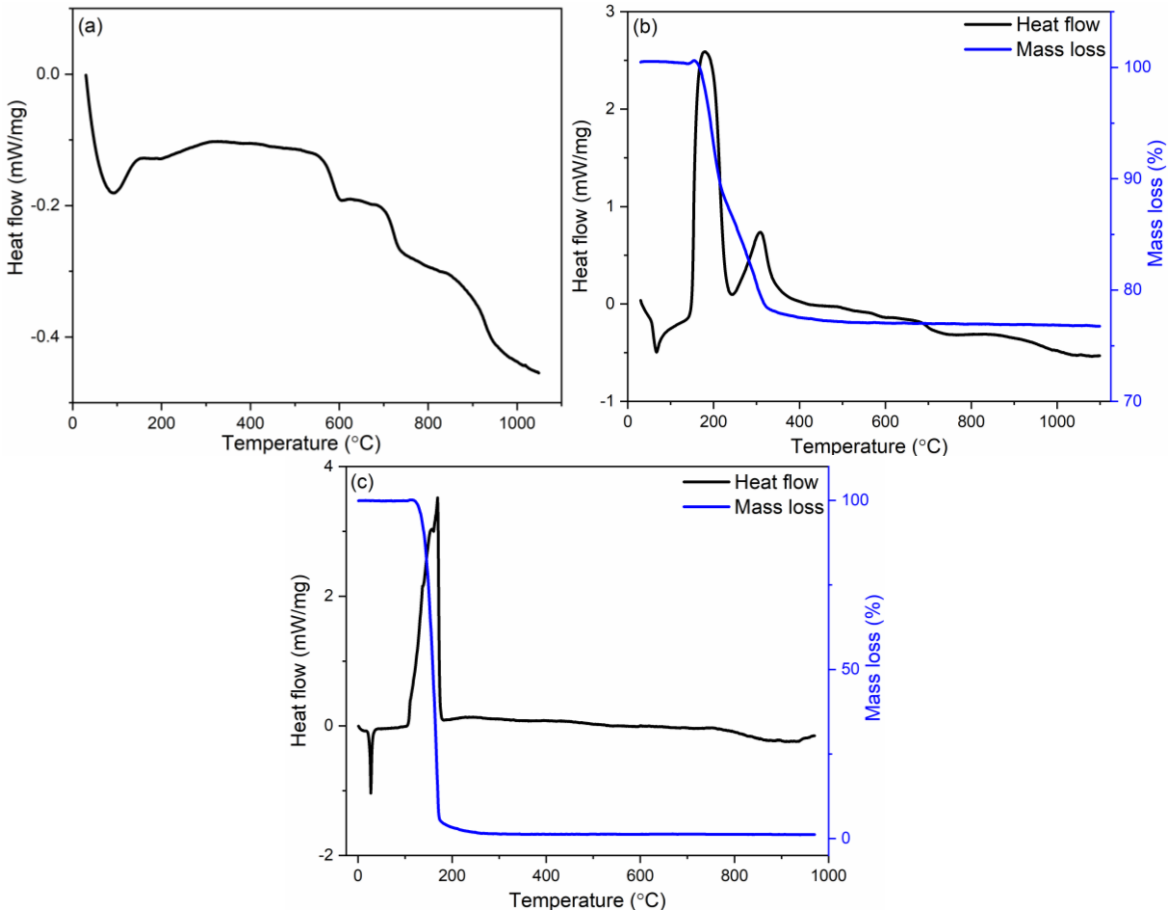


**Figure 7.** DSC/TG curves of borosilicate glass (a), printed sample (b), pure Pluronic F-127 (c)

The green printed samples are shown in Fig. 8a, while samples obtained after the sintering process were still opaque (not shown in Fig. 8a). In order to determine the source of scattering, SEM imaging and X-ray diffraction measurement were performed. Fig. 8b presents a SEM micrograph of fracture surface of sintered glass sample. One can observe that obtained cylinders are highly porous which results in light scattering, while it has a homogeneous appearance. This fact implies that it is still necessary to improve debinding and sintering parameters, or/and instead of processing in air atmosphere, apply vacuum for an effective deairing step.

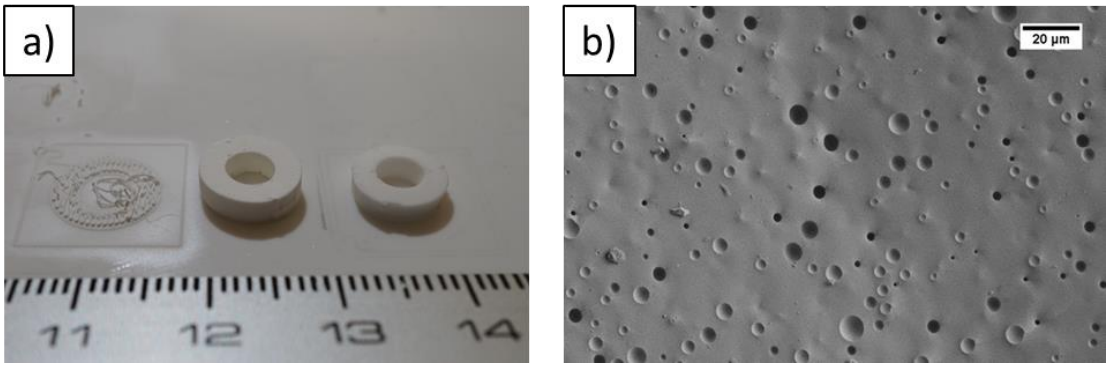


**Figure 8.** (a) Photo and (b) SEM micrograph of printed and sintered glass sample.

Peer-reviewed version available at Materials 2020, 13, 1636; doi:10.3390/ma13071636

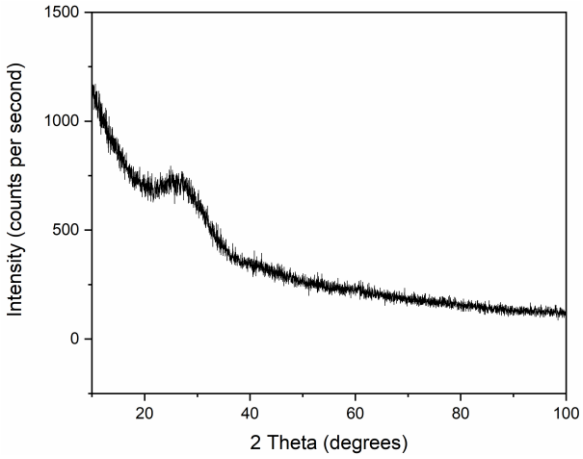


**Figure 9.** XRD pattern of printed and sintered glass sample.

Fig. 9 shows the X-ray diffraction pattern of the sintered sample. This result allows to confirm that after all steps of the manufacturing process, no crystalline phase was developed upon sintering. This result is consistent with the SEM images, where no additional phase was observed. This implies that the proposed manufacturing process is suitable for the preparation of printed transparent glass samples after the implementation of any possible improvements for further densification: in ink mixing process, the composition of inks should be changed in order to increase volume fraction of the glass powder while preserving similar rheological properties so that the green samples should have lower initial porosity. Before printing, an efficient degassing step would be helpful for removing the air bubbles entrapped in the ink. Upon sintering, all the relevant process parameters should be suitably adjusted, and/or further tests exploiting sintering in vacuum should be performed.

## 5. Remarks and conclusions

In this preliminary study, we have successfully 3D printed water-sensitive and micron-sized borosilicate glass with high alkali and alkaline oxide contents by means of direct ink writing. Major difficulties reported in the literature, such as rheological instability of the ink or retaining the shape of the printed object during sintering process, were overcome. The main conclusions are the following:

1. Designed manufacturing process is suitable for obtaining water-sensitive glass inks. Results of rheological measurements showed that inks based on Pluronic F-127 hydrogel are rheologically stable against glass dissolution.

2. Structural analysis after sintering of printed samples showed no crystalline phases introduced during manufacturing process. However, obtained glass rings were opaque. SEM imaging revealed significant amount of closed porosity, which may be responsible for light scattering. In order to obtain more transparent samples, ink composition should be enhanced, additional degassing step added, or/and sintering process improved.

**Author Contributions:** conceptualization, B.N. and P.G.; methodology, P.G. and B.N.; formal analysis, P.G.; investigation, B.N. and P.G.; resources, F.J.G.R., R.B. and J.M.F.F.; writing—original draft preparation, B.N. and P.G.; writing—review and editing, F.J.G.R., R.B. and J.M.F.F.; supervision, F.J.G.R., R.B. and J.M.F.F.; project administration, F.J.G.R., R.B. and J.M.F.F; funding acquisition, F.J.G.R., R.B. and J.M.F.F.

**Funding:** This research was funded by The Polish National Agency for Academic Exchange, grant number PN/BIL/2018/1/00253 and Foundation for Polish Science, grant number POIR.04.04.00-00-1C74/16 (TEAM TECH/2016-1/1). The support received within the scope of the projects FCT Ref. UID/CTM/50011/2019 and POCI-01-531 0145-FEDER-030765, financed by national funds through the FCT/MCTES is also acknowledged.

**Acknowledgments:**

Authors would like to thank Dr Ryszard Stępień from Department of Glass, Institute of Electronic Materials Technology for his support. The facilities from CICECO-Aveiro Institute of Materials, UA, PT; Institute of Electronic Materials Technology, Warsaw, PL, and of Transport Phenomena Research Center (CEFT), FEUP, PT are acknowledged.

**Conflicts of Interest:** The funders had no role in the design of the study; in the collection, analyses, or interpretation of data; in the writing of the manuscript, or in the decision to publish the results.

## References

1. Lee, J. Y.; An, J. Fundamentals and applications of 3D printing for novel materials. *Appl. Mater. Today* **2017,** *7*, 120-133.
2. Lee, J. Y.; Tan, W.S. The potential to enhance membrane module design with 3D printing technology. *J. Memb. Sci.* **2016**, *499*, 480–490.
3. Wong, K.V.; Hernandez, A. A review of additive manufacturing. *ISRN Mech. Eng.* **2012**, *2012*, 1-10.
4. Ngo, T. D.; Kashani, A. Additive manufacturing (3D printing): A review of materials, methods, applications and challenges. *Compos. B Eng.* **2018**, *143*, 172-196.
5. Guo, N.; Leu, M. C. Additive manufacturing: technology, applications and research needs. *Front. Mech. Eng.* **2013**, *8*, 215-243.
6. Truby, R. L.; Lewis, J. A. Printing soft matter in three dimensions. *Nature* **2016**, *540*, 371.
7. Frazier, W. E. Metal additive manufacturing: a review. *J. Mater. Eng. Perform.* **2014**, *23*, 1917-1928.
8. Deckers, J.; Vleugels, J. Additive manufacturing of ceramics: a review. *J. Ceram. Sci. Technol.* **2014**, *5*, 245-260.
9. Chen, Z.; Li, Z. 3D printing of ceramics: A review. *J. Eur. Ceram. Soc.* **2019**, *39*, 661-687.
10. Wang, X.; Jiang, M. 3D printing of polymer matrix composites: A review and prospective. *Compos. B Eng.* **2017**, *110*, 442-458.
11. Gul, J. Z.; Sajid, M. 3D printing for soft robotics–a review. *Sci. Technol. Adv. Mater.* **2018**, *19*, 243-262.
12. Nguyen, D. T.; Meyers, C. 3D-printed transparent glass. *Adv. Mater.* **2017**, *29*, 1701181.
13. Kotz, F.; Arnold, K. Three-dimensional printing of transparent fused silica glass. *Nature* **2017**, *544*, 337.
14. Zhang, J.; Zhao, S. Three-dimensional printing of strontium-containing mesoporous bioactive glass scaffolds for bone regeneration. *Acta Biomater.* **2014**, *10*, 2269-2281.
15. Eqtesadi, S.; Motealleh, A. Robocasting of 45S5 bioactive glass scaffolds for bone tissue engineering. *J. Eur. Ceram. Soc.* **2014**, *34*, 107-118.
16. Destino, J. F.; Dudukovic. 3D printed optical quality silica and silica–titania glasses from sol–gel feedstocks. *Advanced Materials Technologies* **2018**, *3*, 1700323.
17. Moore, D.G.; Barbera, L. Three-dimensional printing of multicomponent glasses using phase-separating resins. *Nat. Mater.* **2019**, 1-6. doi:10.1038/s41563-019-0525-y
18. Klein, J.; Stern, M. Additive manufacturing of optically transparent glass. *3D Print. Addit. Manuf.* **2015**, *2*, 92-105.
19. Luo, J.; Gilbert, L. J. Additive manufacturing of transparent soda-lime glass using a filament-fed process. *J. Manuf. Sci. Eng.* **2017**, *139*, 061006.
20. Vadnere, M.; Amidon, G. Thermodynamic studies on the gel-sol transition of some pluronic polyols. *Int. J. Pharm.* **1984**, *22*, 207-218.
21. Wanka, G.; H. Hoffmann. Phase diagrams and aggregation behavior of poly (oxyethylene)-poly (oxypropylene)-poly (oxyethylene) triblock copolymers in aqueous solutions. *Macromolecules* **1994**, *27*, 4145-4159.
22. Bromberg, L.; Temchenko, M. Bioadhesive properties and rheology of polyether-modified poly (acrylic acid) hydrogels. *Int. J. Pharm.* **2004**, *282*, 45-60.
23. Park, S. Y.; Lee, Y. Temperature/pH-Sensitive Hydrogels Prepared from Pluronic Copolymers End-Capped with Carboxylic Acid Groups via an Oligolactide Spacer. *Macromol. Rapid Commun.* **2007**, *28*, 1172-1176.
24. Marques, C. F.; Perera, F. H. Biphasic calcium phosphate scaffolds fabricated by direct write assembly: Mechanical, anti-microbial and osteoblastic properties. *J. Eur. Ceram. Soc.* **2017**, *37*, 359-368.
25. Nan, B.; Olhero, S. Direct ink writing of macroporous lead-free piezoelectric $Ba_{0.85}Ca_{0.15}Zr_{0.1}Ti_{0.9}O_3$. *J. Am. Ceram. Soc.* **2019**, *102*, 3191-3203.

26. Brazete, D.; Neto, A. S. Optimization of zirconia inks to fabricate 3D porous scaffolds by Robocasting. *Lék. tech. (On-line)* **2019**, *49*, 5-10.
27. Nan, B.; Galindo-Rosales, Francisco J.; Ferreira, J.M.F. 3D printing vertically: Direct ink writing free-standing pillar arrays. *Mater. Today* **2020** (accepted for publication).
28. Feilden, E.; Blanca, E. G. T. Robocasting of structural ceramic parts with hydrogel inks. *J. Eur. Ceram. Soc.* **2016**, *36*, 2525-2533.
29. Dinkgreve, M.; Denn, M.M.; Bonn, D. "Everything flows?": Elastic effects on startup flows of yield-stress fluids. *Rheol. Acta* 2017, 56, 189–194.
30. Hyun, K.; Wilhelm, M. A review of nonlinear oscillatory shear tests: Analysis and application of large amplitude oscillatory shear (LAOS). *Prog. Polym. Sci.* **2011**, *36*, 1697-1753.
31. Hyun, K.; Kim, S. H. Large amplitude oscillatory shear as a way to classify the complex fluids. *J. Nonnewton. Fluid Mech.* **2002**, *107*, 51-65.
32. Mewis, J.; Wagner, N. J. Thixotropy. *Adv. Colloid Interface Sci.* **2009**, *147*, 214-227.
33. Barnes, H. A. Thixotropy—a review. *J. Nonnewton. Fluid Mech.* **1997**, *70*, 1-33.
34. Mewis, J.; De Bleyser, R. Dynamic behavior of thixotropic systems. *J. Colloid Interface Sci.* **1972**, *40*, 360-369.